IEICE TRANS. COMMUN., VOL.E104–B, NO.10 OCTOBER 2021

PAPER

Feasibility Study of Wi-SUN JUTA Profile-Compliant F-RIT Protocol

Ryota OKUMURA[†a)], ***Student Member***, **Keiichi MIZUTANI**[†], ***Member***, ***and*** **Hiroshi HARADA**[†], ***Fellow***

SUMMARY In this paper, the world's first experimental evaluation of the Wi-SUN Japan Utility Telemetering Association (JUTA) profile-compliant feathery receiver-initiated transmission (JUTA F-RIT) protocol is conducted. Firstly, the transmission success rate in an interference environment is evaluated by theoretical analysis and computer simulations. The analysis is derived from the interference model focusing on the carrier sense. The analysis and simulation results agree as regards the transmission success rate of the JUTA F-RIT protocol. Secondly, we develop the dongle-type prototype that hosts the JUTA F-RIT protocol. Measurement results in a cochannel interference environment show that the transmission success rate at the lower MAC layer is around 94% when the number of terminals is 20. When the waiting time for the establishment of the communication link can be extended to exceed 10 s, the JUTA F-RIT protocol can achieve the transmission success rate of over 90% without the re-establishment of the communication link and re-transmission of data frames. Moreover, the experimental results are examined from two viewpoints of the performance of the frame transmissions and the timeout incident, and the feature of the JUTA F-RIT protocol are discussed.

key words: *Wi-SUN, JUTA profile, IEEE 802.15.4, RIT, MAC protocol*

1. Introduction

In the Internet-of-things (IoT) era, various things are being connected to the Internet to collect and utilize a variety of information. A typical IoT system is the smart metering system for electric power infrastructure. In Japan, smart power meters are being introduced widely to gather a huge number of power meter readings automatically and to analyze the electricity usage information in real-time [1], [2]. A fundamental technology for the IoT systems is a wireless communication system that connects a large number of devices to the Internet at low-cost and with high reliability. Cellular-based systems (e.g., narrow-band IoT (NB-IoT) [3]) is one of the solutions. While the NB-IoT can provide highly reliable transmission by operating in licensed bands, a higher service cost is required when all devices communicate directly with a base station by only a cellular-based system. Low-power wide-area (LPWA) systems using unlicensed bands (e.g., industry science and medical (ISM) bands or sub-GHz bands) like the SigFox [4] and the LoRaWAN [5] are also candidates for the IoT systems because they have the advantage of a lower cost than the cellular-based systems. However, these LPWA systems have the drawback that *blind zones* (i.e., no service area due to shadowing effects) are generated in their service range installing in urban areas with dense buildings. To resolve the blind zone problem, the introduction of multi-hop transmissions is necessary. For these reasons, the IEEE 802.15.4-based personal area network (PAN) system supporting multi-hop transmissions is suitable for smart metering in urban areas. In Japan, the 920 MHz-bands are allocated for the smart metering systems [6]; thus, many devices for the smart power meters support the 920 MHz-band operations and the multi-hop transmissions based on the IEEE 802.15.4g-compliant physical (PHY) layer [1], [7].

Similarly, the smart meters have been introduced in gas and water infrastructures (e.g., the wireless M-Bus [8] in Europe). The biggest difference between the smart power meter and the smart gas or water meters is the driving power of the wireless communication device. Generally, the wireless communication device for the smart power meter is driven by a fixed power supply. On the other hand, the device for smart gas or water meters has to be driven by a battery for a long period, such as over ten years. Therefore, media access control (MAC) protocols to operate with low-power consumption have been developed. In the IEEE 802.15.4-2015 [9], several low-power MAC protocols were adopted. The time-slotted channel hopping (TSCH) [10] and the superframe-based MAC protocol [11] can reduce power consumption by introducing a synchronized operation. In contrast, the coordinated sampled listening (CSL) [12] and the receiver-initiated transmission (RIT) [13] do not require synchronization for the low-power operation. These protocols are properly selected according to the requirements of applications. For the Japanese smart metering systems that require ad-hocness for flexible operation, the feathery RIT (F-RIT) protocol has been proposed [13] as an IEEE 802.15.4e RIT-compliant low-power consumption MAC protocol [14]. In [13], the F-RIT-based and the CSL-based protocols were theoretically and numerically evaluated to prove the applicability of the F-RIT-based protocol to the low-power consumption smart metering systems. Furthermore, the authors have developed the world's first Wi-SUN dongle-type prototype, which equipped the F-RIT-based protocol in commercial IEEE 802.15.4g-compliant devices, and feasibility of the protocol was proven by experimental evaluations [15], [16]. Hereafter, the protocol designed and evaluated in [15], [16] is called *the IEEE 802.15.4e-compliant F-RIT protocol*.

For the smart metering system of the city gas, liquefied petroleum (LP) gas, and water infrastructures, the Japan

Manuscript received September 21, 2020.
Manuscript revised January 28, 2021.
Manuscript publicized March 31, 2021.

[†]The authors are with Graduate School of Informatics, Kyoto University, Kyoto-shi, 606-8501 Japan.
a) E-mail: okumura@dco.cce.i.kyoto-u.ac.jp

DOI: 10.1587/transcom.2020EBP3142

Utility Telemetering Association (JUTA) [17] has been developed a Japan domestic wireless communication standard draft named U-Bus Air in 2012 [18], [19]. The U-Bus Air offers reliable multi-hop data transmissions and prolongs its battery-powered operation period by a low-power receiver-initiated asynchronous MAC protocol [20]. The initial U-Bus Air [18] was developed based on the intermittent receiver driven transmission (IRDT) protocol [21], [22]. However, their MAC layer was not compliant with any global standards. To enhance the competitiveness in global markets and to achieve a sustainable device supply, the MAC layer of the initial U-Bus Air had been modified to comply with global standards. The U-Bus Air development team had proposed a lower part of the MAC layer (Low-MAC), and a linking method of the U-Bus Air was standardized as the RIT protocol in the IEEE 802.15.4e [14] in 2012. Also, in 2015, some components of the Low-MAC were adopted in the IEEE 802.15.4-2015 [9]. Finally, the JUTA has standardized the IEEE standard-based PHY layer and Low-MAC to support the U-Bus Air in the Wi-SUN Alliance [23]. This specification is called as the *Wi-SUN JUTA profile*. In this paper, we collectively refer to the protocol designed within the Wi-SUN JUTA profile as *the Wi-SUN JUTA profile-compliant F-RIT protocol*. The Wi-SUN Alliance provides opportunities for certification with the Wi-SUN JUTA profile for newly developed products by testing their interoperability. In the Wi-SUN JUTA profile, the linking method and parameters are newly defined by the IEEE 802.15.4-2015-compliant F-RIT protocol. Also, U-Bus Air systems require the U-Bus Air interface as a higher part than layers defined by the Wi-SUN JUTA profile.

In this paper, the feasibility of the Wi-SUN JUTA profile-compliant F-RIT protocol is studied comprehensively by theoretical analysis, computer simulations, and experiments with developed prototypes. As above-mentioned, the IEEE 802.15.4e-compliant F-RIT protocol was theoretically, numerically, and experimentally evaluated in [13], [15], [16]. However, an evaluation sequence, packet usages, and various parameters in these previous works did not comply with the Wi-SUN JUTA profile and the U-Bus Air standard. Therefore, the Wi-SUN JUTA profile-compliant F-RIT protocol supporting a communication sequence of the U-Bus Air was newly designed in the conference version of this paper [24]. Also, the frame transmission performance was analyzed in [24]. Hereinafter, the protocol evaluated in [24] is called *the JUTA F-RIT protocol*. As an extended work in this paper from [24], the timeout incident is newly analyzed from the simulation and experimental results of the JUTA F-RIT protocol. The key contributions of this paper are the follows:

- We evaluated a transmission success rate of the JUTA F-RIT protocol in a cochannel interference environment by theoretical analysis and computer simulations [24].
- We developed the world's first Wi-SUN dongle-type prototype with the JUTA F-RIT protocol [24]. The commercial dongle equipped with the IEEE 802.15.4g [7] and the ARIB STD-T108 [6] compliant Wi-SUN RF module is used for the implementation.
- By using the developed prototypes, we evaluated the JUTA F-RIT protocol experimentally and demonstrated its feasibility [24].
- We considered the communication performance of prototypes from two viewpoints of the frame transmissions [24] and the timeout incident for the reference of better implementation or upper layer design.

The rest of this paper is organized as follows. The overview of the U-Bus Air communication system based on the Wi-SUN JUTA profile is introduced in Sect. 2. In Sect. 3, theoretical analysis of the JUTA F-RIT protocol is developed. Then, the transmission success rate is evaluated by the analysis and computer simulations for the reference of the performance in the prototype. In Sect. 4, we develop and evaluate the world's first Wi-SUN dongle-type prototype with the JUTA F-RIT protocol. Moreover, the performance of the prototype is considered in detail from the viewpoints of the frame transmissions and the timeout incident. Finally, Sect. 6 concludes this paper.

2. F-RIT Protocol-Based U-Bus Air Communication System

In this section, the U-Bus Air communications system based on the Wi-SUN JUTA profile-compliant F-RIT protocol is explained. In the Low-MAC, the F-RIT protocol defined in the Wi-SUN JUTA profile based on the RIT protocol in IEEE 802.15.4-2015 [9] is adopted. Also, the system adopts the higher part of the MAC layer (High-MAC, i.e., the lower part of the U-Bus Air interface) to achieve the practical communication sequence.

2.1 Overview

The U-Bus Air is the wireless standard for gas and water utilities standardized by the JUTA. The U-Bus Air can accommodate 50 wireless terminals in one mesh network and support multi-hop transmissions with the low-power receiver-initiated MAC protocol for reliable communications.

As explained in Sect. 1, the U-Bus Air was developed based on the IRDT protocol [21] as shown in Fig. 1. The PHY layer of the IRDT was proposed and adopted to the IEEE 802.15.4g [7]. Therefore, the draft of the U-Bus Air released in 2012 [18] adopts the IEEE standard in the PHY layer. However, the whole MAC layer of the IRDT protocol was not related to the IEEE standard. Only a simple and general RIT mechanism (i.e., the RIT protocol explained in the next section) was standardized in the IEEE 802.15.4e [14].

To enhance the competitiveness in global markets, to achieve sustainable device supply, and to ensure the interoperability, the global standardization of the F-RIT protocol with the detailed specifications for the U-Bus Air systems was required. The Wi-SUN JUTA profile [1] defines technical specifications of the PHY and the Low-MAC for the U-Bus Air as shown in Fig. 1. The practical systems require

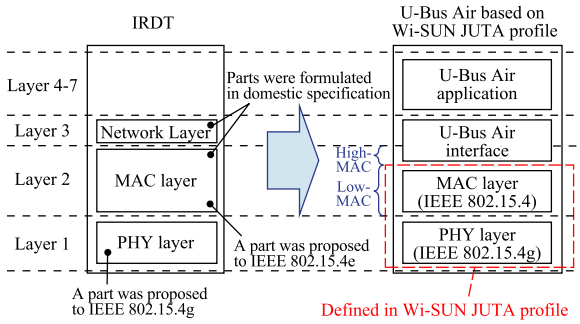

Fig. 1 Standardization for U-Bus Air and typical protocol stack structure with PHY and MAC layers based on Wi-SUN JUTA profile.

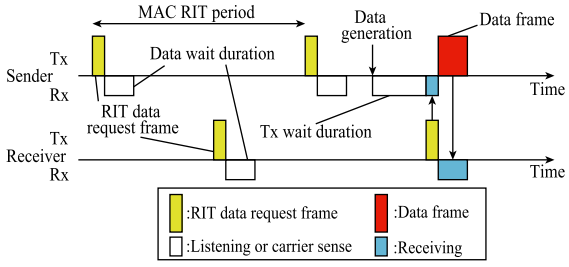

Fig. 2 Procedure of RIT protocol defined in IEEE 802.15.4-2015 [9].

the U-Bus Air interface and applications to offer upper-layer services.

2.2 RIT Protocol in IEEE 802.15.4

The RIT is the protocol that achieves the low-power communications without any synchronization by receiver-initiated communication mechanism. Figure 2 shows the operational procedure of the RIT protocol in the IEEE 802.15.4-2015 [9]. In this protocol, all terminals periodically transmit the RIT data request frame, and the short listening is performed after the transmission to receive frames from other terminals. This transmission interval is called *the MAC RIT period*, and the listening duration is called *the data wait duration* in this paper. If a terminal does not receive any signal from the other terminals, the terminal in the data wait duration gets back to the sleep state until the next wake-up timing.

Let us consider the case that a sender terminal generates a data frame and tries to transmit to a receiver terminal as shown in Fig. 2. In the RIT protocol, the sender starts the listening and waits for the arrival of an RIT data request frame from the destination terminal. This listening state is called as *the Tx wait duration*, and its maximum length is called *the MAC RIT Tx wait duration* in this paper. After the reception of the RIT data request frame from the receiver, the sender transmits the data frame to the receiver. Since the receiver is in the listening state during the data wait duration, it can start to receive the data frame from the sender.

2.3 Wi-SUN JUTA Profile-Compliant F-RIT Protocol

The MAC part of the Wi-SUN JUTA profile supports low-

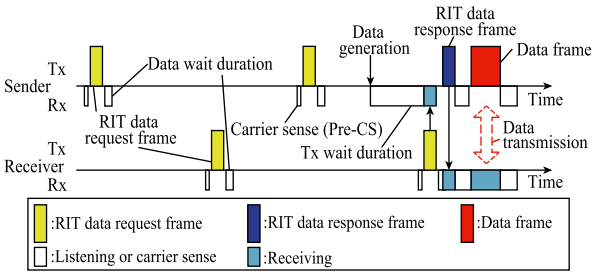

Fig. 3 Communication sequence of F-RIT protocol based on Wi-SUN JUTA profile.

energy data communications based on the IEEE 802.15.4-2015-compliant F-RIT protocol [9]. The F-RIT protocol is an embodying RIT protocol proposed for battery-powered terminals, which has two features [13]. First is the compaction of the RIT data request frame. The RIT data request frame length should be as short as possible to reduce the power consumption and interferences. In the F-RIT protocol, only source terminal information is loaded in an addressing field of the RIT data request frame (i.e., information about the destination terminal is omitted). Second is the simplification of carrier sense multiple access with collision avoidance (CSMA/CA) with a random backoff process to transmit the RIT data request frame. To reduce the power consumption for the transmission of the RIT data request frames in a crowded channel environment, a pre-carrier sense (Pre-CS), which is a simplified channel sampling process, is applied instead of the CSMA/CA process with a random backoff. When a terminal detects another transmission during the period of the Pre-CS, the terminal does not transmit the RIT data request frame until the next periodical wake-up timing.

The Wi-SUN JUTA profile defines three specified frames: an RIT data request frame, an RIT data response frame, and a data frame. The RIT data response frame was newly standardized in the IEEE 802.15.4-2015 [9]. When the RIT data response frame is used, the sender transmits the RIT data response frame in the data wait duration to inform the receiver that the sender is pending a data frame addressed to the receiver as shown in Fig. 3. If the receiver catches the RIT data response frame in the data wait duration, the listening duration is extended. Then, the sender and the receiver can transmit the data frames to each other in this duration.

Figure 4 shows the IEEE 802.15.4-2015-compliant frame structures defined by the Wi-SUN JUTA profile. In the Wi-SUN JUTA profile, the physical service data unit (PSDU) length of all frames should be less than 255 byte. The RIT data request frame shown in Fig. 4(a) loads only the source terminal information in the addressing field in accordance with the specification of the F-RIT protocol. By using the data frame shown in Fig. 4(c) in the Low-MAC, the terminals can achieve various communication processes: an acknowledgement (ACK) or negative ACK for the data transmission request, a transmission of the single or multiple data frames, and a re-transmission of the data frame in the U-Bus Air.

In the JUTA profile, the RIT data request and the data

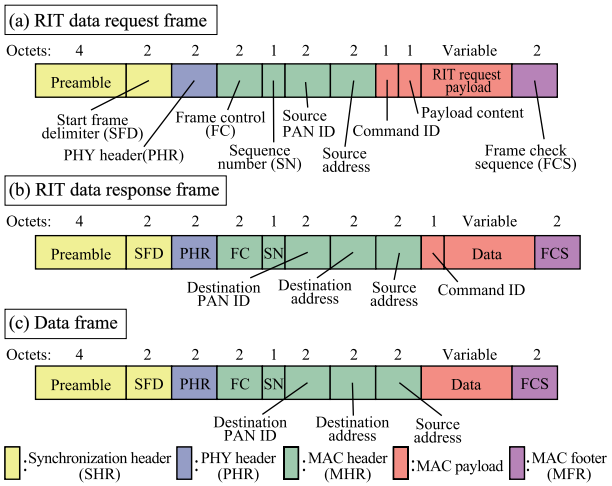

Fig. 4 Detail of frame structures in Wi-SUN JUTA profile.

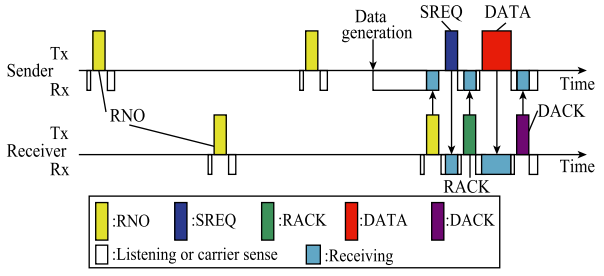

Fig. 5 Major communication sequence in U-Bus Air to transfer data with DATA command.

frames are transmitted after the Pre-CS in the Low-MAC. The action after detecting the channel busy before the transmission of a data frame is issued from the upper layer. The RIT response frame is transmitted without performing the carrier sense so that the receiver can catch the frame within the data wait duration. The Wi-SUN JUTA profile determines some parameters to realize the low-power consumption of the F-RIT protocol within the IEEE standard. For example, the MAC RIT period and the MAC RIT Tx wait duration in the Low-MAC are defined to 5 s. To achieve successful interoperability, the sender should start to transmit the RIT data response frame within the duration from 0.8 ms to 1.25 ms after the reception of the RIT data request frame.

2.4 MAC Layer of U-Bus Air Communication System

The MAC layer of the U-Bus Air defines practical communication sequences using several link control commands for actual services. Figure 5 illustrates the communication sequence which transfers data on a frame with the DATA command. This is a major communication sequence in the U-Bus Air [18], and corresponds to the sequence of the IRDT [21]. In this paper, only the sequence shown in Fig. 5 is considered.

In the Wi-SUN JUTA profile, a radio number (RNO) command and a send request (SREQ) command are applied to the RIT data request frame and the RIT data response frame, respectively. The U-Bus Air defines the acknowledgement for the SREQ command and this is called as a request ACK (RACK) command. The sender transmits the user data on a frame with the DATA command after receiving the RACK command. If the receiver accepts the data, it transmits a DATA ACK (DACK) command to the sender. Hereafter, the frame which loads a certain link control command is called by only the command name (e.g., RNO means the RIT data request frame with the RNO command). In the draft [18], which does not comply with the IEEE standard MAC, RNO and DACK are transmitted with a carrier sense, and SREQ is transmitted without any carrier sense. Here, when a carrier is detected by the carrier sense, re-transmission is not performed. RACK and DATA are transmitted using the carrier sense, which waits for the carrier to be clear state for a certain period if it detects a carrier. Besides this normal sequence, the U-Bus Air defines various communication processes that are required in actual services. For example, the receiver can refuse the request for the communication link establishment by transmitting the request negative ACK (RNACK). Moreover, the sender can re-transmit the DATA if it does not receive DACK. Furthermore, not only single DATA transmission, but also the multiple DATA transmissions, and the bidirectional exchange of the DATA are supported.

3. Theoretical Analysis and Evaluation of JUTA F-RIT Protocol

In this section, the JUTA F-RIT protocol is designed as a Wi-SUN JUTA profile-compliant F-RIT protocol for evaluations. The performance of the JUTA F-RIT protocol is evaluated by theoretical analysis and computer simulations for references of experiments in the next section. Theoretical analysis is derived from the analysis scheme focusing on the carrier sense proposed in [24].

3.1 System Model

In this paper, we consider the one-way communication model in an interference environment as illustrated in Fig. 6. In the system model with N terminals, one specific terminal (i.e., sender) generates the data and transmits to a specific terminal (i.e., receiver) based on the JUTA F-RIT protocols. Other $N-2$ terminals do not transmit any data, namely, they transmit only RIT data request frames which acts as interferences. All terminals are operated in a single channel. In this system model, the transmission performances are evaluated under cochannel interferences of only RIT data request frames. This model can be considered as a part of a snapshot of the multi-hop polling communication from the center terminal coordinating a network, which is a function of the U-Bus Air [19].

To randomize the timing of the data generation, the next data generation timing is decided at the end of the data transmission operation. We define the interval of the data

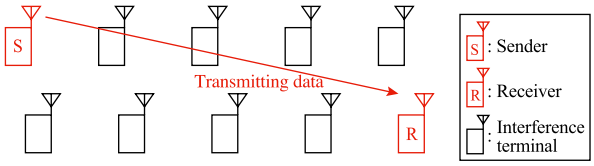

Fig. 6 System model.

transmission operation as the data generation interval, and the reciprocal numbers of the intervals follow to the Poisson distribution in this paper. The MAC RIT period is not absolutely fixed and slightly randomized in the simulation in Sect. 3.5 since the actual modules are affected by the clock drift [25], and the RIT data request frames are not transmitted at intervals of the ideal MAC RIT period.

In this paper, since we focus on the communication in the MAC layer, especially in the Low-MAC, only the PHY and the Low-MAC are implemented in the actual module evaluated in Sect. 4. Therefore, we assume that the data frames are transmitted from the High-MAC on the outside of the module as a minimum setup of the Wi-SUN JUTA profile, and the communication delay between the High-MAC and the Low-MAC based on the universal asynchronous receiver/transmitter (UART) is considered in the simulation.

3.2 Practical JUTA F-RIT Protocol for Evaluation

To evaluate the practical protocol with the features of the Wi-SUN JUTA profile in the Low-MAC, we designed the practical JUTA F-RIT protocol for the evaluation [24]. In this paper, the typical communication sequence of the U-Bus Air, which is shown in Fig. 5 and designed based on the Wi-SUN JUTA profile, is considered.

The range of the MAC RIT Tx wait duration is set in the range from 5 to 25 s. Although the MAC RIT Tx wait duration is defined as same as the MAC RIT period evaluated in [13], [15], [16], the U-Bus Air sets the listening duration waiting for the RNO as a guide as 5 times of the RNO transmission interval [18]. This means the RIT-based system with the High-MAC waits for the communication chances for several times of the RIT data request frame transmission from the receiver in the High-MAC. Taking the specification of the U-Bus Air that has the whole MAC layer into account, the MAC RIT Tx wait duration over 5 s can be applied in the Low-MAC.

In the communication sequence for the evaluation, we consider two steps for the successful communication as enabling the MAC RIT Tx wait duration over the MAC RIT period in the Low-MAC. The first step is the establishment of a communication link (i.e., the receiver and the sender receive SREQ and RACK, respectively). During the Tx wait duration, the sender attempts to establish the communication link and waits for the reception of the RNO from the receiver until the successful communication link establishment. The second step is the successful execution of the communication link that the sender receives DACK and accomplishment of the communication link. If the communication sequence

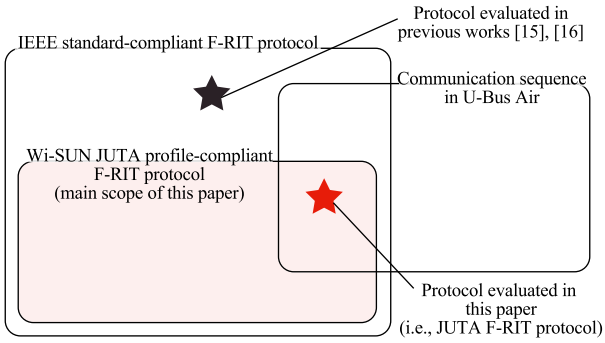

Fig. 7 Relationship between standards and protocols.

stops in the second step, the communication pair do not try to establish the communication link again after one successful communication link establishment because we focus on the evaluation of the Low-MAC. During the link establishment, the re-transmission of the data frame is also not performed.

Figure 7 summarizes the relationship between standards and protocols for evaluations mentioned in this paper. Since the Wi-SUN JUTA profile complied with the IEEE standards, the Wi-SUN JUTA profile-compliant F-RIT protocol should be included in the IEEE standard-compliant F-RIT protocol. Regardless of these international standards, we can also consider the communication sequence of the U-Bus Air. Although the IEEE 802.15.4e-compliant F-RIT protocol was included in the IEEE standard-compliant F-RIT protocol, it did not comply with the Wi-SUN JUTA profile and was not designed based on the communication sequence of the U-Bus Air. The main scope of this paper is the Wi-SUN JUTA profile-compliant F-RIT protocol. The JUTA F-RIT protocol is designed within the Wi-SUN JUTA profile and supports the communication sequence in the U-Bus Air.

3.3 Interference Model and Analysis of Frame Transmissions

In this section, the frame transmissions are analyzed based on the interference model shown in Fig. 8 [24]. The interference model considers frame transmissions in interference environments of RIT data request frames. At the same time, as the generation of the desired frame (i.e., the RIT data request or data frames), the terminal starts the carrier sense. At the Pre-CS, the channel state is assessed at the center of the sensing duration T_{CS}. If the channel state is clear, the terminal starts transmitting the frame after the Rx to Tx turnaround time T_{TA} from the end of the Pre-CS.

As shown in Fig. 8, the result of the transmission of the desired frame depends on the generation of interference frames. For simplicity of the analysis, we do not consider the generation of multiple interference RIT data request frames during the desired frame transmission process. In the system model, the probability that an interference RIT data request frame is generated during the duration of t is $(N-2)/T_{RIT} \cdot t$. Here, T_{RIT} denotes the MAC RIT period (i.e., the generation interval of the RIT data request frame at a terminal).

As illustrated in Fig. 8(a), the carrier is detected at the

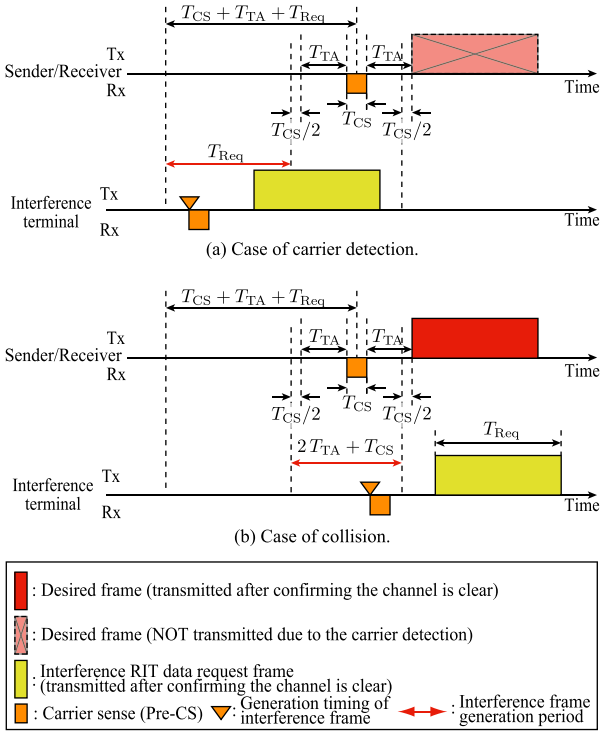

Fig. 8 Interference model for analysis of frame transmissions.

Pre-CS if an interference frame is generated during the RIT data request frame length T_{Req}. Hence, the theoretical incident rate of carrier detection is described as follows:

$$p_{Detect} = \frac{N-2}{T_{RIT}} \cdot T_{Req}. \tag{1}$$

When an interference frame is generated during $2T_{TA}+T_{CS}$ as illustrated in Fig. 8(b), the sender or receiver cannot detect the carrier at the Pre-CS. In this case, the desired frame transfer fails because the collision occurs between the desired frame and an interference RIT data request frame. The theoretical incident rate of the collision is expressed by

$$p_{Collision} = \frac{N-2}{T_{RIT}} \cdot (2 \cdot T_{TA} + T_{CS}). \tag{2}$$

The transfer of the desired frame succeeds in the case that the carrier is not detected at the Pre-CS, and also the collision does not occur. Therefore, the probability of the successful transfer of the desired frame is expressed by

$$p_{wCS} = \left(1 - \frac{N-2}{T_{RIT}} \cdot T_{Req}\right) \cdot \left(1 - \frac{N-2}{T_{RIT}} \cdot (2T_{TA} + T_{CS})\right). \tag{3}$$

In the case that the desired frame is the RIT data response frame, only the collision case should be considered because the carrier sense is not performed as explained in Sect. 2.3. The collision occurs when the interference terminal performs the carrier sense at the duration that starts at the end of the RIT data request frame transmitted by the receiver and the start of the RIT data response frame transmitted by the sender. We define the turnaround time of the sender from the end of the reception of an RIT data request frame to the start of the transmission of an RIT data response frame as the RIT data response Tx ON T_{TxON}. The probability that the receiver catches the RIT data response frame successfully is described as follows:

$$p_{woCS} = 1 - \frac{N-2}{T_{RIT}} \cdot T_{TxON}. \tag{4}$$

3.4 Theoretical Analysis of JUTA F-RIT Protocol

In this section, the communication performance of the target JUTA F-RIT protocol is derived based on the analysis of frame transmissions in the previous section. In the JUTA F-RIT protocol, the communication link is established when transfers of RIT data request frame (i.e., RNO), RIT data response frame (i.e., SREQ), and RACK succeed continuously as described in Sect. 3.2. Hence, the communication link establishment success probability for one trial is described as follows:

$$p_{Link} = p_{wCS} \cdot p_{woCS} \cdot p_{wCS}. \tag{5}$$

Then, if DATA and DACK transfers succeed continuously after the establishment of the communication link, the link results in successful execution. Therefore, the probability of successful execution of the communication link is expressed by

$$p_{Exec} = p_{wCS} \cdot p_{wCS}. \tag{6}$$

In the JUTA F-RIT protocol described in Sect. 3.2, we assume that the communication pair may have multiple chances (i.e., the number of timings to receive the RIT data request frames from the receiver may larger than one) to establish the communication link. The transmission success rate for n times of chances to establish the communication link is expressed by

$$p_{Suc}(n) = \begin{cases} 0, & (n=0) \\ \left\{\sum_{k=0}^{n-1} (1-p_{Link})^k\right\} \cdot p_{Link} \cdot p_{Exec}. & (n \geq 1) \end{cases} \tag{7}$$

Here, the chances to establish the communication link depend on MAC RIT Tx wait duration T_{TWD} (i.e., the maximum duration that the sender waits for the RIT data request frame from the receiver). n is expressed by $\lfloor T_{TWD}/T_{RIT} \rfloor$ or $\lfloor T_{TWD}/T_{RIT} \rfloor + 1$ for the probabilities of $1 - (T_{TWD}/T_{RIT} - \lfloor T_{TWD}/T_{RIT} \rfloor)$ and $T_{TWD}/T_{RIT} - \lfloor T_{TWD}/T_{RIT} \rfloor$, respectively. Therefore, the transmission success rate is expressed as follows with the MAC RIT Tx wait duration T_{TWD}:

$$\begin{aligned} p_{Suc,T_{TWD}} = {} & p_{Suc}\left(\left\lfloor \frac{T_{TWD}}{T_{RIT}} \right\rfloor\right) \cdot \left\{1 - \left(\frac{T_{TWD}}{T_{RIT}} - \left\lfloor \frac{T_{TWD}}{T_{RIT}} \right\rfloor\right)\right\} \\ & + p_{Suc}\left(\left\lfloor \frac{T_{TWD}}{T_{RIT}} \right\rfloor + 1\right) \cdot \left(\frac{T_{TWD}}{T_{RIT}} - \left\lfloor \frac{T_{TWD}}{T_{RIT}} \right\rfloor\right). \end{aligned} \tag{8}$$

Table 1 Parameters for evaluation.

Parameter	Values
Wireless transmission rate	100 kbit/s
Number of terminals N	10–50
RIT data request frame length (RNO command)	28 byte
RIT data response frame length (SREQ command)	25 byte
Data frame length (RACK command)	22 byte
Data frame length (DATA command)	250 byte
Data frame length (DACK command)	22 byte
MAC RIT period T_{RIT}	5 s
Data generation interval	30 s
MAC RIT Tx wait duration T_{TWD}	5–25 (s)
Pre-CS length T_{CS}	0.13 ms
Rx to Tx turnaround time T_{TA}	0.19 ms
RIT data response Tx ON T_{TxON}	0.8 ms
Long interframe spacing (LIFS)	1 ms
Baudrate	115200 baud

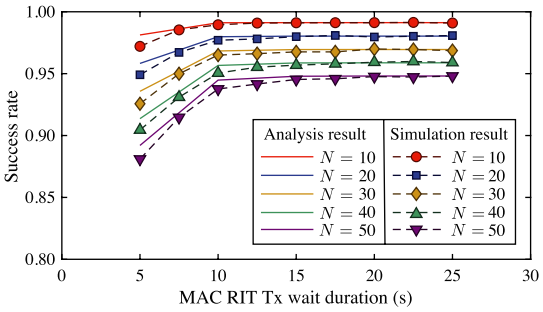

Fig. 9 Transmission success rate characteristics by theoretical analysis and computer simulations.

3.5 Evaluation of Transmission Performance

The transmission success rate characteristics of the JUTA F-RIT protocol is evaluated by theoretical analysis and computer simulations. The simulator is developed originally by the authors using MATLAB. In the simulator, frames are generated and transmitted following the system model and the protocol design explained in Sects. 3.1 and 3.2, respectively. Table 1 shows the parameters for the evaluation. The protocol is evaluated in several numbers of terminals N and MAC RIT Tx wait durations T_{TWD}. In a communication system including upper layers, DATA may contain accumulated user data and routing data. Therefore, assuming a large data size within the 255 byte PSDU length limit specified by the Wi-SUN JUTA profile, we set a frame length of 250 byte, which is the same as in the past evaluations of the IEEE 802.15.4e-compliant F-RIT protocol [15], [16]. The data generation interval is set to only 30 s. This is a value to evaluate the basic communication performances, although it is high frequency compared to the actual communication traffic generation for smart metering systems. In the system model, only RIT data request frames are interference from the viewpoint of the communication pair. In other words, the transmission success rate is not affected by the data generation interval. To allow more trials in the experiments explained in Sect. 4.2, a small interval is set. Therefore, the same value is set in the computer simulations. In the computer simulations, the process delays which appear in the actual prototypes are considered. The Rx to Tx turnaround time is given based on the ideal specification of the module and firmware used in the prototype described in Sect. 4.1. Following the assumption mentioned in Sect. 3.1 that considers the implementation, the delay between the reception and the transmission of frames (e.g., the delay at the sender after receiving RACK until transmitting DATA) is considered in the computer simulations. This assumes the waiting duration for UART communications between the Low-MAC and the High-MAC with the baudrate of 115200 baud. The number of transmission trials is set to 1.0×10^5 for each parameter in computer simulations. The transmission is judged as success when the sender receives DACK successfully.

Figure 9 shows the transmission success rate characteristics of the JUTA F-RIT protocols as a function of the MAC RIT Tx wait duration T_{TWD}. Both of the theoretical analysis results and the computer simulation results have similar characteristics: the transmission success rate tends to converge to a certain rate for each number of terminals as the MAC RIT Tx wait duration T_{TWD} extends. The chance to establish the communication link is given once when the MAC RIT Tx wait duration $T_{\mathrm{TWD}}$is set equal to the MAC RIT period T_{RIT}, and the chance may fail due to the interference of RIT data request frames. By extending the MAC RIT Tx wait duration, the chance to establish the communication link increases. However, the transmission success rate does not approach 100% since the re-transmission of data frames and re-establishment of the communication link is not performed in this evaluation focusing on the Low-MAC. In both of the analysis results and the simulation results, the JUTA F-RIT protocol can achieve the transmission success rate of about 95% when the MAC RIT Tx wait duration T_{TWD} is 5 s and the number of terminals N is 20, that is the typical interference condition of smart metering [16].

Although the theoretical analysis and the simulation results show a similar tendency, there is some divergence when the MAC RIT Tx wait duration T_{TWD} is small. This is because the timings to transmit RIT data request frames are described independently every time during the MAC RIT period in the analysis, while the RIT data request frames are transmitted in an interval in the practical protocol. On the other hand, the deviations between the theoretical analysis and the simulation results are within 0.1% when the MAC RIT Tx wait duration T_{TWD} is 25 s. This means that the analysis of the frame transmissions has high accuracy.

4. Development of Prototype and Experimental Evaluation of JUTA F-RIT Protocol

In this section, we develop the world's first actual Wi-SUN dongle-type prototype that hosts the JUTA F-RIT protocol and evaluate its transmission performance experimentally.

4.1 Development of Prototype and Experimental Configuration

The Wi-SUN dongle-type prototype is developed by the

Table 2 Specification of Wi-SUN dongles.

Items	Specifications
USB dongle	ROHM Co., Ltd BP35C2
RF module	ROHM Co., Ltd BP35C0
Baud rate	115200 baud
Wireless standard	Based on ARIB STD-T108 [6]
Modulation	2-Gaussian frequency shift keying (GFSK)
Wireless frequency	920 MHz band
Transmission rate	100 kbit/s
Transmission power	20 mW
Receiving sensitivity	–103 dBm (TYP.) (100 kbit/s, BER<0.1%)

commercial USB-type Wi-SUN dongle installing the JUTA F-RIT protocol [24]. The commercial Wi-SUN dongle (BP35C2, ROHM Co., Ltd.) with the specification shown in Table 2 is used for the development. In the dongle, IEEE 802.15.4g-compliant [7] and Wi-SUN alliance-certified [23] radio module (BP35C0, ROHM Co., Ltd.) is integrated. The firmware that works as Low-MAC in the RF module and the application that acts as simple High-MAC for the evaluation on the PC are developed to evaluate the JUTA F-RIT protocol. The developed dongles are connected to the PC via USB cables and controlled by the application on the PC. In the implemented protocol, the RIT data request and RIT data response frames are transmitted from the Low-MAC in the module, and data frames are transmitted from the High-MAC on the PC application. The connection between the High-MAC on the PC and Low-MAC on the module is based on UART communication. In the developed protocol, there is no synchronization or clock correction between dongles. The protocol is implemented so that some parameters related to frame transmission timings (e.g, the Rx to Tx turnaround time, the RIT data response Tx ON, and the LIFS) are realized around the values shown in Table 1. The data wait duration starts 0.7 ms after the transmission of the RIT data request frame and continues for 1.2 ms. This is to ensure that the RIT data response frame is received correctly even if there is some variance in the RIT data response Tx ON in the prototypes.

In an experimental configuration shown in Fig. 10, N terminals are placed in a plane of 50 cm × 12 cm. The system model is as same as shown in Fig. 6, and the two dongles placed in a diagonal position of the plane are the sender and the receiver. Others are interference terminals since all terminals are operating in a single channel. This experimental configuration is designed to evaluate the basic transmission performance as similar as in Sect. 3. In this environment, the sender or the receiver is located farther away from each other than any other interference terminal. This is to prevent the received power of the desired frame from being sufficiently larger than the received power of the interference frame. In other words, the dongles are arranged so that the collision likely occurs if the desired and the interference frames are transmitted simultaneously as assumed in Sect. 3.

4.2 Experimental Evaluation Results

The parameters of the experimental evaluation are shown in Table 3. The number of trials of communications for each

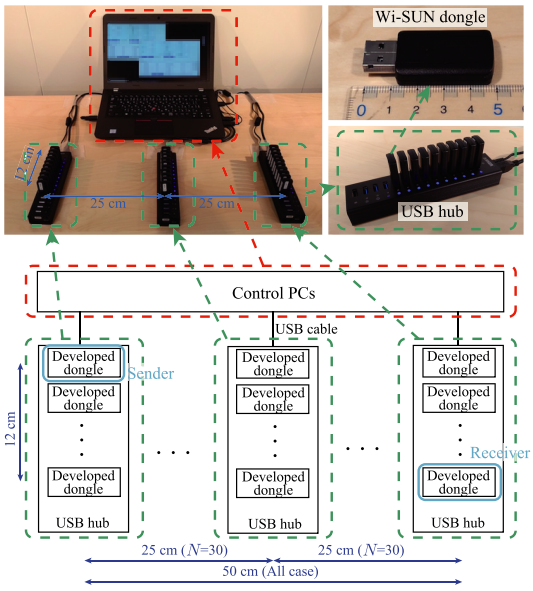

Fig. 10 Configuration of experiments (N = 30).

Table 3 Parameters of experimental evaluation.

Parameter	Values
Wireless frequency	923.7, 925.7, 927.7 (MHz)
Number of terminals N	10–50
RIT data request frame length (RNO command)	28 byte
RIT data response frame length (SREQ command)	25 byte
Data frame length (RACK command)	22 byte
Data frame length (DATA command)	250 byte
Data frame length (DACK command)	22 byte
MAC RIT period T_{RIT}	5 s
Average data generation interval	30 s
MAC RIT Tx wait duration T_{TWD}	5–25 (s)
Pre-CS length T_{CS}	0.13 ms

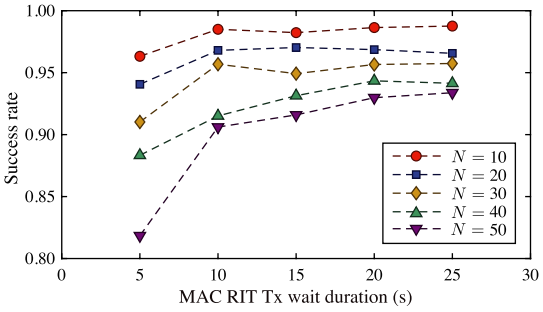

Fig. 11 Experimental results of transmission success rate.

parameter is 1.0×10^4. Figure 11 shows the measurement results of the transmission performances as a function of the MAC RIT Tx wait duration T_{TWD}. The measured transmission success rate is calculated from the ratio of successful receptions of DACK for the communication trials. When the MAC RIT Tx wait duration T_{TWD} is set to 5 s, which is the specified value of the JUTA profile in the Low-MAC, the JUTA F-RIT protocol can achieve the transmission success rate of over 90% in cases of N = 10, 20, 30. When N =20, the transmission success rate of around 94% is achieved. As the MAC RIT Tx wait duration T_{TWD} is prolonged, the trans-

mission success rate tends to converge to a certain rate for each number of terminals (e.g., the transmission success rate of around 98.5% in the case of $N = 10$). When the MAC RIT Tx wait duration T_{TWD} is set to 25 s, the transmission success rate over 90% is achieved without the re-establishment of the communication link and re-transmission of data frames in all cases of numbers of terminals N. The measurement results of the transmission success rate show a tendency similar to the simulation results discussed in Sect. 3.5, while the differences between the measurement results and the simulation results are within 5.0%.

5. Consideration of Performances in Prototype

In this section, the transmission performances in prototypes are considered in detail to provide the reference for better implementation or upper layer design. Focusing mainly on the Low-MAC, we discuss the transmission performance of data frames and the timeout incident.

5.1 Frame Transmission Performance

It is important to understand the frame transmission performance in the Low-MAC because the backoff is omitted in the Wi-SUN JUTA profile. Especially the results of the Pre-CS before transmitting data frames may be utilized for the link control of the protocol (e.g., re-transmission of data frames) controlled from the upper layer. Note that the main aim of this paper is to grasp the performance in the Low-MAC for the upper layer design, and the impact of the link control design in the High-MAC is out of the scope of this paper.

In this section, the transmission performances of data frames with the DATA and DACK commands are discussed from the theoretical analysis and the experimental results. As discussed in Sect. 3.3, the incident rate of the carrier detection and the incident rate of the collision are calculated from Eqs. (1) and (2), respectively. In the experiments in Sect. 4, the transmission results of data frames with the DATA and DACK commands can be obtained from the information reported to the application (i.e., the numbers of transmission trials, carrier detections, and successful receptions).

Figures 12 and 13 show the incident rate characteristics of carrier detection and the collision, respectively. Theoretically, both characteristics increase linearly to the amount of interference (i.e., the number of terminals N). While there is some deviation between the theoretical analysis results and experimental results that may be caused by processing delay in actual modules, the experimental results show a similar tendency with the theoretical analysis in both incident rates of the carrier detection and the collision. For example, when the number of terminals N is 50, the collision occurs with probability from 0.34% to 0.64% in the experimental results, while the rate is 0.49% in the theoretical result as shown in Fig. 13. Such incident rates of the collision are not small that cannot be ignored compared to the incident rates of the carrier detection, which occur from 2.4% to 3.4% in experimental results as shown in Fig. 12.

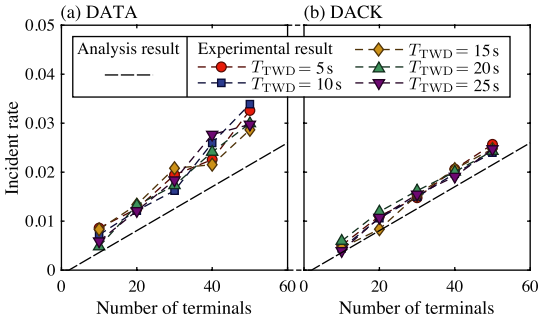

Fig. 12 Incident rate of carrier detection.

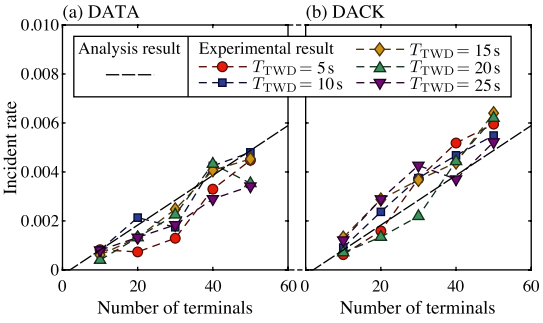

Fig. 13 Incident rate of collision.

From the above results, it is shown that the collision frequently occurs with a high probability of around one-fifth of the case of the carrier detection in theoretically in the JUTA F-RIT protocol at the Low-MAC, where the most of air traffic are occupied by short and frequently transmitted RIT data request frames. Therefore, it is preferable to design the upper layer on the assumption that collisions will occur frequently.

5.2 Timeout Incident

In this section, the transmission characteristics of the JUTA F-RIT protocol are discussed with regard to the RIT unique timeout problem. Comparing Figs. 9 and 11, it can be found that the transmission success rate shows that the measured transmission success rate is lower than the simulation results. Also, the transmission performances of data frames after the establishment of the communication link cannot be the main reason for the deterioration in the experimental results because the performance can be explained from a theoretical approach as discussed in Sect. 5.1. Mainly, the reason for the deterioration in the experimental results is the timeout problem, which occurs in the process of establishing the communication link. The timeout is one of the major causes of transmission failures in RIT-based systems that occurs when the sender does not receive the RIT data request frame from the receiver during the Tx wait duration [16].

Figure 14 shows the incident rate of the timeout as a function of the MAC RIT Tx wait duration T_{TWD} in the simulation and the experimental results. In the simulation results, the MAC RIT period is slightly randomized intentionally in

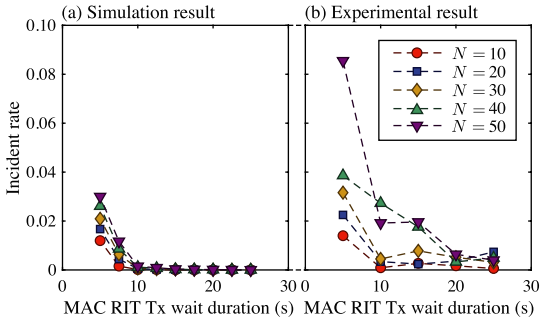

Fig. 14 Comparison of incident rate of timeout in simulation and experimental results.

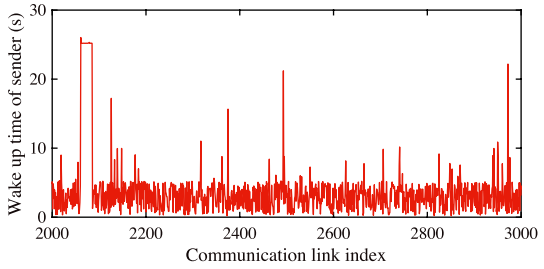

Fig. 15 Example of experimental result of wake-up time of sender.

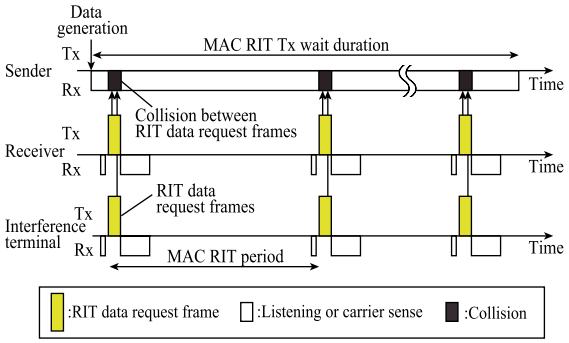

Fig. 16 Mechanism of timeout incident due to continuous collision between RIT data request frames.

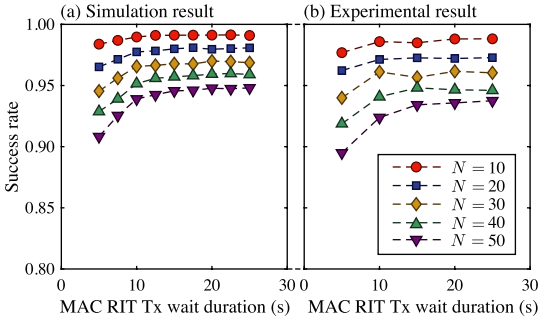

Fig. 17 Comparison of the simulation and experimental results of the transmission success rate excluding case of timeout.

the simulator. On the other hand, the MAC RIT period deviates in actual modules by clock variations. Therefore, the MAC RIT period is affected by individual specificity. Furthermore, the clock is affected by temperature fluctuations. In such a condition, the timeout incidents in the experiment are not simply discussed.

To discuss the timeout problem in actual modules, an example of the wake-up duration characteristics of a sender for several communication links is shown in Fig. 15. This example is obtained when the MAC RIT Tx wait duration T_{TWD} is 25 s, and the number of terminals N is 20. In this example, the wake-up durations are around 25 s at the communication link index (i.e., the index of trials at the sender) from 2,061 to 2,085. In this period, the sender cannot receive RIT data request frames from the receiver due to the collision with interference frames from a specific terminal as shown in Fig. 16. Such continuous collisions sometimes occur, and the incident rate of timeout in the measurement results is higher than the simulation results. Due to the bias of the continuous timeout incident, the success rate depending on the parameters does not make sufficiently clear in the experimental results. Figure 17 shows the simulation and the experimental results of the transmission success rate that exclude the timeout incident from the number of trials. The degradation of the transmission success rate from the simulation results due to causes other than the timeout is evaluated from these characteristics. The differences in the transmission success rate are within 1.5%. The deterioration of the frame transmission performance described in Sect. 5.1 can be considered a reason for the differences in the transmission success rate, excluding timeout.

In this way, continuous collisions, which is the problem unique to the RIT protocol, may cause continuous timeouts in the actual devices. This problem cannot be detected by the carrier sense and can occur over a longer period of time if the terminal has a high-accuracy clock. Therefore, it is preferable to take measures such as periodically resetting the initial timing to transmit the RIT data request frames in consideration of the timeout problem.

6. Conclusion

In this paper, we conducted the world's first experimental evaluation of the JUTA F-RIT protocol. Firstly, the transmission success rate in an interference environment was evaluated by theoretical analysis and computer simulations. It was shown that the theoretical analysis and simulation showed a similar tendency on the transmission performance of the JUTA F-RIT protocol. Then, we developed the world's first Wi-SUN dongle-type prototype that hosts the JUTA F-RIT protocol. The experimental results in the interference environment showed that the transmission success rate at the Low-MAC was around 94% when the specification of the JUTA profile was given, and the number of terminals was 20. When the waiting time for the establishment of the communication link was extended over 10 s, the JUTA F-RIT protocol can achieve the transmission success rate of over 90% without the re-establishment of the communication link and re-transmission of data frames. Moreover, the frame transmission performances and the timeout incident in

the prototype were discussed in detail to provide references for better implementation and upper layer design.

Acknowledgments

The authors would like to thank Dr. J. Fujiwara and Mr. T. Kawata of Tokyo Gas Co., Ltd. for useful discussions. A part of this work was funded by ImPACT Program of Council for Science, Technology and Innovation (Cabinet Office, Government of Japan). A part of this work was supported by Grant-in Aid for JSPS Research Fellow Grant Number JP18J23198 and the MIC/SCOPE #196000002.

References

[1] H. Harada, K. Mizutani, J. Fujiwara, K. Mochizuki, K. Obata, and R. Okumura, "IEEE 802.15.4g based Wi-SUN communication systems," IEICE Trans. Commun., vol.E100-B, no.7, pp.1032–1043, July 2017.
[2] K. Akabane, N. Mochizuki, S. Teruhi, M. Kobayashi, S. Yoshino, M. Shimizu, and K. Uehara, "High-capacity wireless access networks using 920 MHz band for wide-area IoT/M2M services," IEICE Trans. Commun., vol.E99-B, no.9, pp.1920–1929, Sept. 2016.
[3] M. Chen, Y. Miao, H. Yixue, and K. Hwang, "Narrow band Internet of things," IEEE Access, vol.5, pp.20557–20577, Sept. 2017.
[4] A. Lavric, A.I. Petrariu, and V. Popa, "Long range SigFox communication protocol scalability analysis under large-scale, high-density conditions," IEEE Access, vol.7, pp.35816–35825, March 2019.
[5] F. Adelantado, X. Vilajosana, P. Tuset-Peiro, B. Martinez, J. Melia-Segui, and T. Watteyne, "Understanding the limits of LoRaWAN," IEEE Commun. Mag., vol.55, no.9, pp.34–40, Sept. 2017.
[6] Association of Radio Industries and Business, "920 MHz-band telemeter, telecontrol and data transmission radio equipment ARIB STD-T108 version 1.3," April 2019.
[7] IEEE Computer Society, "IEEE Std 802.15.4g™-2012," April 2012.
[8] M. Carratù, M. Ferro, V. Paciello, A. Pietrosanto, and P. Sommella, "Performance analysis of wM-Bus networks for smart metering," IEEE Sensors J., vol.17, no.23, pp.7849–7856, Dec. 2017.
[9] IEEE Computer Society, "IEEE Std 802.15.4™-2015," Dec. 2012.
[10] A. Karaagac, J. Haxhibeqiri, W. Joseph, I. Moerman, and J. Hoebeke, "Wireless industrial communication for connected shuttle systems in warehouses," Proc. IEEE WFCS 2017, pp.1–4, May 2017.
[11] F. Kojima and H. Harada, "Superframe division multi-hop data collection with aggregation on Wi-SUN profile for ECHONET lite," Proc. IEEE WCNCW, pp.116–121, April 2014.
[12] K. Samejima, R. Okumura, K. Mizutani, and H. Harada, "Evaluation of CSL-based low power MAC protocol for wireless smart metering networks," Proc. IEEE CCNC 2020, pp.1–6, Jan. 2020.
[13] J. Fujiwara, H. Harada, T. Kawata, K. Sakamoto, S. Tsuchiya, and K. Mizutani, "An ultra-low power consumption MAC protocol complied with IEEE 802.15.4/4e for wireless smart utility networks," IEEJ Trans. EIS, vol.137, no.11, pp.1555–1566, Nov. 2016 (in Japanese).
[14] IEEE Computer Society, "IEEE Std 802.15.4e™-2012," April 2012.
[15] J. Fujiwara, R. Okumura, K. Mizutani, and H. Harada, "Feasibility study of F-RIT low-power MAC protocol complied with IEEE 802.15.4/4e for wireless smart utility network," IEEJ Trans. EIS, vol.137, no.11, pp.1461–1471, Nov. 2017 (in Japanese).
[16] R. Okumura, J. Fujiwara, K. Mizutani, and H. Harada, "Enhancd F-RIT protocol for wireless smart utility networks with high traffic bi-directional communications," IEICE Trans. Commun., vol.E101-B. no.12, pp.2487–2497, Dec. 2018.
[17] Japan Utility Telemetering Association, http://www.teleme-r.or.jp/index.html
[18] Japan Utility Telemetering Association, "U-bus air communications specification draft ver. 2.0," June 2012 (in Japanese).
[19] Japan Utility Telemetering Association, "U-bus air functions specification draft ver. 1.1," Aug. 2012 (in Japanese).
[20] H. Hayashi, "Evolution of next-generation gas metering system in Japan," Proc. IEEE IMS2014, pp.1–4, Sept. 2014.
[21] D. Kominami, M. Sugano, M. Murata, and T. Hatauchi, "Energy-efficient receiver-driven wireless mesh sensor networks," Sensors, vol.11, no.1, pp.111–137, Dec. 2011.
[22] T. Hatauchi, Y. Fukuyama, M. Ishii, and T. Shikura, "A power efficient access method by polling for wireless mesh network," IEEJ Trans. EIS, vol.128, no.12, pp.1761–1766, Dec. 2008 (in Japanese).
[23] Wi-SUN Alliance, https://www.wi-sun.org
[24] R. Okumura, K. Mizutani, and H. Harada, "Analysis and experimental verification of F-RIT protocol for wireless smart utility network," Proc. IEEE CCNC 2019, pp.1–6, Jan. 2019.
[25] Y. Kawamoto, T. Matsunaga, and Y. Kado, "MAC protocol with clock synchronization correction for a practical infrastructure monitoring system," International Journal of Distributed Sensor Networks, vol.14, no.4, pp.1–14, April 2018.

Ryota Okumura is a candidate of a Ph.D. degree of Graduate School of Informatics, Kyoto University, Japan. From 2018, he is a Research Fellow DC1 at Japan Society for the Promotion of Science (JSPS). He received a B.E. degree in electric and electrical engineering from the Kyoto University in 2016, and an M.I. degree in communications and computer engineering from the Kyoto University in 2018. He currently researches the topics of physical and media access control layers of wireless smart utility networks (Wi-SUN). He received IEEE VTS Tokyo Chapter Student Encouragement Award from IEEE VTS Tokyo Chapter in 2017 and The Telecom System Technology Student Award from The Telecommunication Advancement Foundation in 2019.

Keiichi Mizutani is an associate professor at Kyoto University. He received a B.E. degree in electric, electrical and system engineering from the Osaka Prefecture University in 2007, and an M.E. and Ph.D. degree in electric and electrical engineering from the Tokyo Institute of Technology in 2009 and 2012 respectively. He was an invited researcher at Fraunhofer Heinrich Hertz Institute, Germany, in 2010. From April 2012 to Sept. 2014, he was a researcher at NICT, and from Oct. 2014 to Dec. 2020, he was an assistant professor at Kyoto University. He currently researches physical layer technologies in white space communications, dynamic spectrum access, and the 5G and Beyond 5G access technologies. He received the Special Technological Award and Best Paper Award from IEICE SR technical committee in 2009 and 2010, respectively, the Young Researcher's Award from IEICE SRW technical committee in 2016, WPMC 2017 Best Paper Award, and WPMC 2020 Best Paper Award. Dr. Mizutani is a member of the IEEE.

Hiroshi Harada is a professor of the Graduate School of Informatics, Kyoto University. He joined the Communications Research Laboratory, Ministry of Posts and Communications, in 1995 (currently, NICT). Since 1995, he has researched software defined radio, cognitive radio, dynamic spectrum access network, wireless smart ubiquitous network, and broadband wireless access systems on the microwave and millimeter-wave band. He also has joined many standardization committees and forums in the United States as well as in Japan and fulfilled important roles for them, especially IEEE 1900 and IEEE 802. He was the chair of IEEE DySpan Standards Committee and a vice chair of IEEE 802.15.4g, IEEE 802.15.4m, 1900.4, and TIA TR-51. He was a board of directors of IEEE communication society standards board, SDR forum, DSA alliance, and WhiteSpace alliance. He is a co-founder of Wi-SUN alliance and has served as the chairman of the board from 2012 to 2019. He is currently the Vice chair of IEEE 2857, IEEE 802.15.4aa and Wi-SUN alliance. He moreover was the chair of the IEICE Technical Committee on Software Radio (TCSR) and the chair of Public Broadband Mobile Communication Development Committee in ARIB. He is also involved in many other activities related to telecommunications. He has authored the book entitled Simulation and Software Radio for Mobile Communications (Artech House, 2002). He received the achievement awards in 2006 and 2018 and fellow of IEICE in 2009, respectively and the achievement awards of ARIB in 2009 and 2018, respectively, on the topic of research and development on software defined radio and wireless smart utility network.